



**HAL**  
open science

## Salinity Assessment for Salted Soil Considering Both Dissolved and Precipitated Salts

Zi Ying, Yu-Jun Cui, Nadia Benahmed, Myriam Duc

► **To cite this version:**

Zi Ying, Yu-Jun Cui, Nadia Benahmed, Myriam Duc. Salinity Assessment for Salted Soil Considering Both Dissolved and Precipitated Salts. *Geotechnical Testing Journal*, 2021, pp.1-10. 10.1520/GTJ20190301 . hal-03114283

**HAL Id: hal-03114283**

**<https://hal.science/hal-03114283>**

Submitted on 28 May 2021

**HAL** is a multi-disciplinary open access archive for the deposit and dissemination of scientific research documents, whether they are published or not. The documents may come from teaching and research institutions in France or abroad, or from public or private research centers.

L'archive ouverte pluridisciplinaire **HAL**, est destinée au dépôt et à la diffusion de documents scientifiques de niveau recherche, publiés ou non, émanant des établissements d'enseignement et de recherche français ou étrangers, des laboratoires publics ou privés.



Distributed under a Creative Commons Attribution - NonCommercial - NoDerivatives 4.0  
International License



Contents lists available at ScienceDirect

# Journal of Rock Mechanics and Geotechnical Engineering

journal homepage: [www.jrmge.cn](http://www.jrmge.cn)

Full Length Article

## Salinity effect on the compaction behaviour, matric suction, stiffness and microstructure of a silty soil

Zi Ying<sup>a</sup>, Yu-Jun Cui<sup>a,\*</sup>, Nadia Benahmed<sup>b</sup>, Myriam Duc<sup>c</sup><sup>a</sup> Ecole des Ponts ParisTech, Laboratoire Navier/CERMES, 6-8 av. Blaise Pascal, Cité Descartes, Champs-sur-Marne, Marne-la-Vallée cedex 2, 77455, France<sup>b</sup> INRAE, Aix Marseille Univ, RECOVER, Equipe G2DR, 3275 route Cézanne, CS 40061, Aix-en-Provence, 13182, France<sup>c</sup> Université Gustave Eiffel, IFSTTAR/GERS/SRO, 14-20 boulevard Newton, Champs-sur-Marne, Marne-la-Vallée, 77447, France

## ARTICLE INFO

## Article history:

Received 4 August 2020

Received in revised form

4 January 2021

Accepted 19 January 2021

Available online xxx

## Keywords:

Silts

Compaction

Suction

Stiffness

Microstructure

## ABSTRACT

To better understand the salinity effect on the compaction behaviour of soil, standard Proctor compaction test was conducted on soil samples with different salinities. Matric suction and small-strain shear modulus,  $G_{max}$ , were determined and pore size distribution was also investigated on samples statically compacted at different water contents. Results showed that with the decrease of soil salinity from initial value of 2.1‰ (g of salt/kg of dry soil) to zero, the maximum dry density increased and the optimum water content decreased, whereas there was no significant change with the increase of soil salinity from 2.1‰ to 6.76‰. Interestingly, it was observed that  $G_{max}$  also decreased when the soil salinity decreased from initial value of 2.1‰ to zero and kept almost constant when the soil salinity increased from 2.1‰ to 6.76‰, for dry samples with similar matric suction and also for samples compacted at optimum state and on wet side whose matric suctions were slightly different due to the difference in remoulded water content. Furthermore, the effect of salinity on compaction behaviour and  $G_{max}$  decreased for samples compacted from dry side to wet side. The pore size distribution exhibited bi-modal characteristics with two populations of micro- and macro-pores not only for samples compacted on dry side and at optimum state, but also for those compacted on wet side. Further examination showed that the modal size of micro-pores shifted to lower values and that of macro-pores shifted to higher values for saline soil compared to the soil without salt.

© 2021 Institute of Rock and Soil Mechanics, Chinese Academy of Sciences. Production and hosting by Elsevier B.V. This is an open access article under the CC BY-NC-ND license (<http://creativecommons.org/licenses/by-nc-nd/4.0/>).

### 1. Introduction

For the economic and environmental reasons, it is recommended to use local soils in geotechnical and geo-environmental constructions such as subgrades, dikes, dams and municipal waste barriers. In coastal area, soil pore water normally contains certain salinity, which can greatly affect the compaction behaviour of soils. Liu and Zhang (2014) reported that both the maximum dry density and optimum water content decreased with increasing salinity for saline soils with 3%–8% clay-size fraction. Nevertheless, Ajalloeian et al. (2013) indicated that salinity had negligible effect on the compaction behaviour of fine-grained soils with 28% clay-size fraction. Abdullah et al. (1997, 1999) stated that the salt solution led to an increase in maximum dry density and a reduction of

optimum water content for highly plastic clay whose main minerals were illite and smectite. The same observations were made on clayey soils with 48% clay minerals consisting of montmorillonite, polygorskite and kaolinite (Abood et al., 2007) and on expansive soils (Shariatmadari et al., 2011; Durotoye et al., 2016). They attributed this phenomenon to the decrease of diffused double layer thickness and the more oriented face-to-face clay particle contacts with the increase of salinity. From these studies, it appears that the salinity had different effect on compaction properties for soils with different clay fractions and mineral compositions. On the whole, the maximum dry density increased and the optimum water content decreased with increasing salinity for clays which had high clay fraction and swelling minerals, whereas the salinity had no significant effect on compaction behaviour or led to reductions of

\* Corresponding author.

E-mail address: [yu-jun.cui@enpc.fr](mailto:yu-jun.cui@enpc.fr) (Y.-J. Cui).

Peer review under responsibility of Institute of Rock and Soil Mechanics, Chinese Academy of Sciences.

<https://doi.org/10.1016/j.jrmge.2021.01.002>1674-7755 © 2021 Institute of Rock and Soil Mechanics, Chinese Academy of Sciences. Production and hosting by Elsevier B.V. This is an open access article under the CC BY-NC-ND license (<http://creativecommons.org/licenses/by-nc-nd/4.0/>).

Please cite this article as: Ying Z et al., Salinity effect on the compaction behaviour, matric suction, stiffness and microstructure of a silty soil, Journal of Rock Mechanics and Geotechnical Engineering, <https://doi.org/10.1016/j.jrmge.2021.01.002>

**Table 1**  
Geotechnical properties of the tested soil.

Property	Unit	Value
Specific gravity, $G_s$		2.72
Liquid limit, $w_L$	%	29
Plastic limit, $w_p$	%	19
Plasticity index, $I_p$	%	10
Value of methylene blue of soil (VBS)	g/100 g	0.98
Specific surface area (SSA)	m <sup>2</sup> /g	24

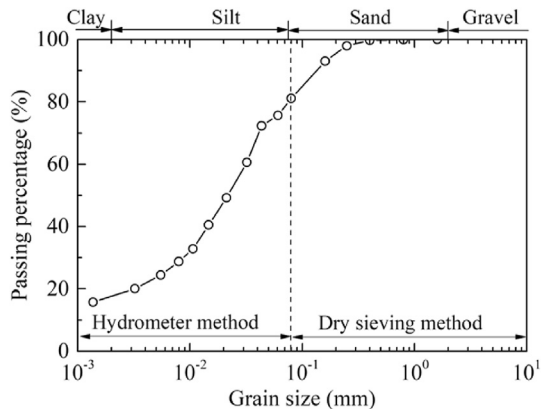


**Fig. 1.** Grain size distribution of natural soil.

both maximum dry density and optimum water content for soils with low clay fraction.

Salt can also significantly influence the strength or stiffness of compacted soils. Recent studies mainly focused on the strength variations with salinity changes (Abood et al., 2007; Ajalloeian et al., 2013; Zhang et al., 2013a; Carteret et al., 2014; Liu and Zhang, 2014). Some studies focused on the effect of salinity on the stiffness of illite (Witteveen et al., 2013) and cemented soils (Truong et al., 2012; Zhang et al., 2013b). It was reported that the unconfined compressive strength increased with increasing salinity for soils with a fraction of clay minerals as large as 48% (Abood et al., 2007) and for saline soils with only 3%–8% clay-size fraction (Liu and Zhang, 2014). Liu and Zhang (2014) explained that the increased shear strength for saline soils was due to the salt crystal cementation of soil particles which improved soil mechanical behaviour. As for the samples with high quantity of clay minerals, the thickness of diffused double layer decreased with increasing salinity and this, in turn, caused repulsive force diminution and net attractive force increase (Mitchell and Soga, 2005; Israelachvili, 2011). The increased net attractive force enabled soil particles to associate with each other in an aggregated manner, which may enhance soil strength (Moore, 1991; Di Maio et al., 2004; Tiwari et al., 2005; Abood et al., 2007). In addition to salinity effect, it was also reported that the stiffness of soil increased with the increase of matric suction but at a declining rate (Ng and Yung, 2008; Ng et al., 2009; Heitor et al., 2013). However, salinity had no significant effect on matric suction which was related to the capillary and hydration forces (Miller and Nelson, 1993; Leong et al., 2007; Sreedeeep and Singh, 2011).

**Table 2**  
Chemical analysis of natural soil pore water.

Chemical compositions (mg/L) (ICP/AES method)								Salt concentration, $c$ (g/L)	Soil salinity, $r'$ (‰ or g salt/kg of dry soil)
Cl	Na	Ca	K	Mg	Fe	Al	Si		
7521	5096	215	225	176	18	7	39	13.3	2.1

Concerning the correlations between microstructure and mechanical behaviour, several studies focused on the salinity effect on microstructure variations. Carteret et al. (2014) performed scanning electron microscope (SEM) and mercury intrusion porosimetry (MIP) tests on compacted saline samples with different salinities. They observed that the salt crystallisation of highly saline samples caused reduction of macro-pores and increase of meso- and micro-pores, and these salt crystals were found to form bonds among soil particles which led to the increase of soil strength. Zhang et al. (2013a) also observed some salt bonding between clay particles of loess on SEM images, and this bonding resulted in aggregation of particles, increasing the shear strength. Sarkar and Siddiqua (2016) conducted X-ray computed tomography (X-ray CT) test on bentonite-sand materials prepared by distilled water and salt solutions, and highlighted the salt effect on pore size distribution properties of compacted samples: the pore size and number of interconnected pores increased with increasing salinity due to the reduction of diffused double layer thickness.

It appears from the above-mentioned studies that the salinity effect on compaction behaviour, matric suction, stiffness or microstructure was conducted on different soils. However, there were few studies focusing on all these different properties of a given soil. In this study, standard Proctor compaction test was first conducted on soil samples with different salinities. To further understand the salinity effect on soil compaction behaviour, filter paper method, bender element test and MIP test were carried out on samples compacted on dry side, at optimum state and on wet side. Results allowed the coupled compaction behaviour, matric suction, stiffness and microstructure to be analysed.

## 2. Materials and methods

### 2.1. Tested materials

Natural saline silty soil was taken from Salin-de-Giraud, a traditional salt exploitation site in France. Its geotechnical properties are reported in Table 1. Fig. 1 shows the grain size distribution of the soil, which was determined by the dry sieving method for particles larger than 80  $\mu$ m and by the hydrometer method for particles smaller than 80  $\mu$ m, according to the French standards NF P94-057 (1992) and NF P94-056 (1996), respectively. This soil consists of 20% sand, 63% silt-size particles (0.002–0.075 mm) and 17% clay-size fraction (<0.002 mm). The main minerals, identified by X-ray diffraction (XRD) analysis, are quartz (39%), calcite (35%), feldspar (9.5%), illite (10.8%), chlorite (3.6%), kaolinite (1.3%) and NaCl crystallized on halite form (0.8%). The quantity of clay minerals (illite, chlorite and kaolinite) is 15.7%, in agreement with the clay-size fraction of 17% observed on grain size distribution curve.

Soil solutions were extracted by centrifugation method after several cycles of washing. The chemical compositions and ion concentration of soil solution extracts were determined by inductively coupled plasma/atomic emission spectroscopy (ICP/AES). As listed in Table 2, the ion concentration of soil solution extracts was transformed to ion concentration of soil pore water according to the dilution ratio. The salt concentration of soil pore water was estimated at about 13.3 g/L. Since the salt concentration of soil pore water always changed with water content variations, the soil

**Table 3**  
Chemical compositions of synthetic sea water.

Salt	Salt mass (g) in 1 kg deionised water	Percentage (%)
NaCl	30	70.26
MgCl <sub>2</sub> ·6H <sub>2</sub> O	6	14.05
MgSO <sub>4</sub> ·7H <sub>2</sub> O	5	11.71
CaSO <sub>4</sub> ·2H <sub>2</sub> O	1.5	3.51
KHCO <sub>3</sub>	0.2	0.47

salinity, defined as the ratio of salt mass to dry soil mass, was adopted in this study. For the tested soil, the soil salinity was found to be 2.1‰ (g of salt/kg of dry soil).

## 2.2. Soil salinity adjustment

Since the main ion species of soil pore water were Cl<sup>-</sup>, Na<sup>+</sup>, Ca<sup>2+</sup>, K<sup>+</sup> and Mg<sup>2+</sup>, the same as the ion compositions of synthetic sea water (French standard NF P18-837 (1993), as listed in Table 3), five different salts of synthetic sea water were chosen for preparing the mixed salt solution to be added to the natural saline soil in order to obtain saline soil with higher salinity. The quantity of additive salt was determined according to the initial salinity of natural saline soil and the target salinity of saline soil (Ying et al., 2021). The total additive salt mass was adjusted to each salt mass according to the proportions of the five different salts in synthetic sea water. Mixed salt solution was prepared by dissolving the five additive salts in deionised water. Afterwards, salt solution was sprayed to natural soil in layers to reach the desired soil salinities of about 4.83‰ (or g of salt/kg of dry soil) and 6.76‰, respectively. Note that the maximum target soil salinity of 6.76‰ corresponded to the salt concentration of soil pore water of 35 g/L (salt concentration of synthetic sea water) for saline soil at 20% water content.

To decrease the salinity of natural saline soil, leaching tests were carried out. Leaching column was filled with natural soil. Then, deionised water, with a water head of 1 m, was flushed through the column from bottom to top in order to remove the initial salt (Fig. 2). The water flow rate was controlled to be lower than 0.3 mL/s, preventing the migration of fine particles and avoiding the destruction of soil aggregates. To minimise as much as possible the soil disturbance during leaching, a layer of gravel, geotextile and filter paper were placed on the top and bottom surfaces of the soil.

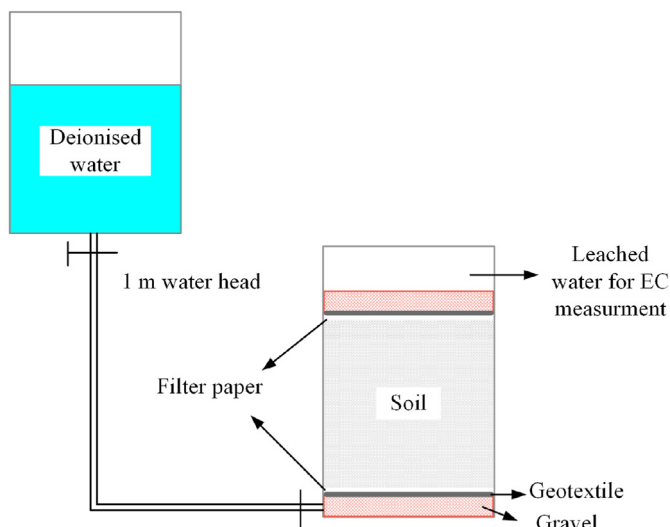


**Fig. 2.** Sketch of the equipment for salt leaching experiment.

The effluent was collected and electrical conductivity (EC) was measured to verify whether the salt was washed out. The leaching of soil was repeated until the amount of salt, thus the EC, was reduced considerably. When the EC of leaching water was close to the one of deionised water and kept almost constant, the test was stopped and a small quantity of leached soil was taken out to verify the final soil salinity. A value as low as 0.05‰ was obtained, which could be regarded as zero. The natural soil, saline soil and leached soil were then air-dried, ground and sieved through 5 mm mesh. The larger soil particles which could not pass through the 5 mm sieve were ground again and rescreened until the whole soils passed through the sieve (Tang et al., 2011).

## 2.3. Sample preparation

Air-dried soil was humidified by spraying deionised water to reach different target water contents on dry and wet sides and at optimum state, and then stored in sealed plastic bag for 24 h aiming at salt and water homogenization. Afterwards, the samples were reconstituted either by dynamic compaction for Proctor test or by static compaction for the matric suction and small-strain shear modulus measurements as well as for the microstructure investigation. For these cases of static compaction, the samples were reconstituted at the target dry density using double pistons acting at the top and bottom of the soil samples to ensure uniform distribution of stresses inside the sample, hence, a better soil homogeneity with respect to the dry density (Cui and Delage, 1996). The samples for matric suction measurement and MIP test had dimensions of 50 mm in diameter and 20 mm in height, and the samples for small-strain shear modulus measurement had 50 mm in diameter and 50 mm in length.

## 2.4. Proctor compaction test

Standard Proctor compaction tests were conducted following the French standard NF P94-093 (1999). Air-dried soil was prepared with the procedure presented previously. Deionised water was then added into the soil to reach different water contents. At each water content, the soil was dynamically compacted in three layers into Proctor mould, with 25 blows of the hammer for each layer. The compacted sample was trimmed by means of a straightedge scraping across the top of the mould. The density of compacted sample ( $\rho$ ) was then determined considering the sample mass and the mould volume. A portion of sample was taken for water content determination.

When a saline sample was dried in an oven, the water evaporated but the salt remained with dry soil (Noorany, 1984). Thus, the water content ( $w$ ) computed from the conventional equation (Eq. (1)) was not equal to the water content ( $w'$ ) of saline soil, which was the ratio of salty water mass ( $m_{sw}$ ) to dry soil mass ( $m_s$ ):

$$w = \frac{m_w}{m_d} \quad (1)$$

where  $m_w$  is the pure water mass and  $m_d$  is the solid mass after oven-drying which contained total mass of soil and salt.

The water content of saline soil ( $w'$ ) should be calculated by Eq. (2) taking the dissolved salt into account (Noorany, 1984; ASTM D4542-95(2001), 2001; Ying et al., 2021):

$$w' = \frac{m_{sw}}{m_s} = \frac{m - m_d}{m_d - rm} \quad (2)$$

where  $r$  is the water salinity, expressed as the mass ratio of salt to salty water; and  $m$  is the wet soil mass.

To convert the salinity on the soil basis to the solution basis, the following equation was adopted (Reitemeier, 1946; Ying et al., 2021):

$$r = \frac{r'}{w'} \quad (3)$$

where  $r'$  is the soil salinity on the basis of dry soil mass.

Then, the dry density ( $\rho_d$ ) for saltless soil can be calculated as

$$\rho_d = \frac{\rho}{1 + w} \quad (4)$$

However, for saline soil, the dry density calculated by Eq. (4) was overestimated because of the consideration of the dissolved salt as soil solids. Thus, the dry density of saline soil should be calculated by Eq. (5) (Noorany, 1984; ASTM D4542-95(2001), 2001; Siddiqua et al., 2011):

$$\rho'_d = \frac{\rho}{1 + w'} \quad (5)$$

The degree of saturation ( $S_r$ ) of compacted samples can be determined from the water content and dry density:

$$S_r = \frac{w\rho_d G_s}{\rho_w G_s - \rho_d} = \frac{wG_s}{\rho_w(G_s/\rho_d - 1)} \quad (6)$$

where  $\rho_w$  is the liquid density.

Finally, based on the values of dry density and water content, the Proctor compaction curves of saltless soil and saline soil with different soil salinities were plotted. The compaction states on dry and wet sides of optimum and at optimum water content with

target dry densities were selected to prepare samples for matric suction, small-strain shear modulus and microstructure investigations.

## 2.5. Matric suction measurement

Matric suction of soil sample was determined by filter paper method, according to ASTM D5298-10 (2010). Whatman No. 42 filter paper was oven-dried for at least 16 h prior to use in the measurements. Three stacked filter papers were sandwiched between two soil samples. The central filter paper used for matric suction measurement was slightly smaller in diameter than the outer filter papers, preventing the central filter paper from direct contact with soil. The entire sandwiched samples were wrapped by plastic film and enveloped by scotch tape. Then, they were stored in a chamber at a relative humidity of 100% and a temperature of  $(20 \pm 2)^\circ\text{C}$  to allow moisture equilibration for two weeks. After equilibration, the water contents of soil sample and central filter paper were measured.

According to ASTM D5298-10 (2010), the following equations of Whatman No. 42 filter paper calibration curves were used to transform the water content of filter paper to matric suction of soil sample:

$$\log_{10}\phi_m = \begin{cases} 5.327 - 0.0779w_f & (w_f \leq 45.3\%) \\ 2.412 - 0.0135w_f & (w_f > 45.3\%) \end{cases} \quad (7)$$

where  $\phi_m$  is the matric suction of soil sample (kPa), and  $w_f$  is the water content of filter paper (%). Note that the mean values of matric suction and water content on the two replicated measurements were considered.

## 2.6. Bender element test

The bender element technique was used to measure the small-strain shear modulus. The set-up of bender elements and a schematic diagram are shown in Fig. 3. This system consists of two piezo-ceramic bender elements, a function generator, an amplifier and an oscilloscope (Wang et al., 2017, 2020; Zhang et al., 2018).

Immediately after compaction, the samples were carefully covered by paraffin to avoid water evaporation. Then, a slot was performed on the surface of the sample extremities with the same direction to install the piezo-ceramic elements and ensure a good contact with soil. The sample was then placed on a wooden holder for a good insulation and for avoiding any signal electrical perturbation (Fig. 3a). Hereafter, a simple pulse was generated by the function generator and amplified by the amplifier. The S + P method proposed by Wang et al. (2017) was adopted to determine the arrival time of shear wave ( $\Delta t$ ). In the S + P method, both transmitted and received signals were captured by the oscilloscope through modifying the connection between the two benders (Fig. 3b). The shear wave velocity ( $v_s$ ) was calculated by

$$v_s = \frac{L_{tt}}{\Delta t} \quad (8)$$

where  $L_{tt}$  is the travel length or tip-to-tip distance between two bender elements.

Finally, the small-strain shear modulus ( $G_{\max}$ ) was determined by

$$G_{\max} = \rho v_s^2 \quad (9)$$

To check the reproducibility of tests, the  $G_{\max}$  measurement was determined in duplicate, and the mean value was used in this study.

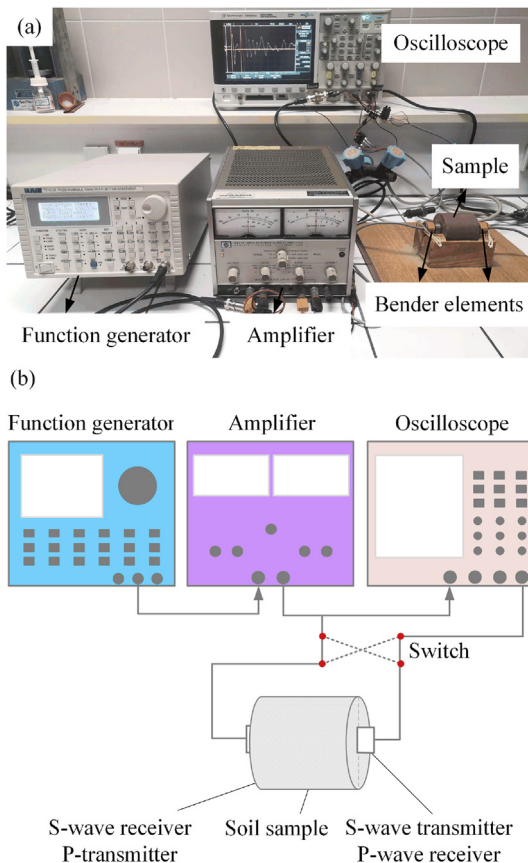


Fig. 3. Set-up of bender element test: (a) Photo of the set-up; and (b) Sketch of the set-up (after Wang et al., 2017).

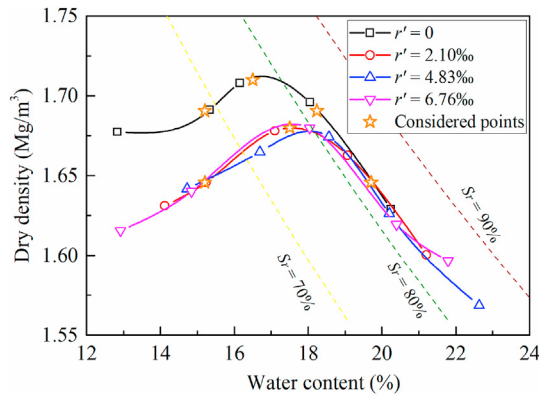


Fig. 4. Salinity effect on Proctor compaction behaviour.

2.7. Microstructure investigation

Autopore IV 9500 mercury intrusion porosimeter was used to investigate the microstructure of compacted samples. After compaction, one small piece of soil was carefully cut from the sample, and then frozen using liquid nitrogen under vacuum and dried using a freeze dryer for 24 h aiming at sublimation of frozen water. To perform the MIP test, the freeze-dried piece was firstly put into a low pressure system with a pressure range varying from 3.6 kPa to 200 kPa, and then transferred to a high pressure system with the maximum pressure of 230 MPa. The corresponding detectable entrance pore diameter ranged from 0.006 μm to 350 μm.

3. Results

3.1. Proctor compaction behaviour

The results of the Proctor compaction curves for soil without salt and those with different soil salinities are depicted in Fig. 4. It can be observed that, with decreasing soil salinity from initial value of 2.1‰ to zero, the compaction curve moved upwards and leftwards, implying that the saltless soil had higher maximum dry density and lower optimum water content than that of natural soil with soil salinity of 2.1‰. However, as soil salinity increased from 2.1‰ to 4.83‰ and 6.76‰, the compaction curves did not exhibit distinguishable changes: the saline soil samples with different salinities had rather close values of maximum dry densities and optimum water contents. Comparison between Proctor compaction curves of saltless soil and saline soils suggested that the salt had more significant effect on the compaction curves on dry side than that on wet side.

The properties of the compacted samples used for matric suction, small-strain shear modulus and microstructure investigations are given in Table 4. The corresponding points are shown in Fig. 4. All the considered compaction states were located on the Proctor compaction curves. Note that the same compaction pressure of about 2200 kPa was recorded for all samples. Note also that for a

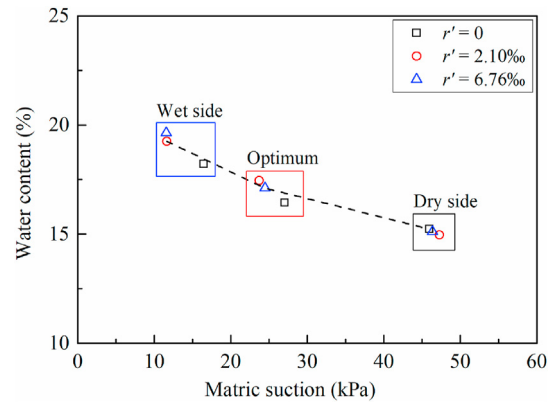


Fig. 5. Matric suction of compacted samples on dry and wet sides and at optimum state.

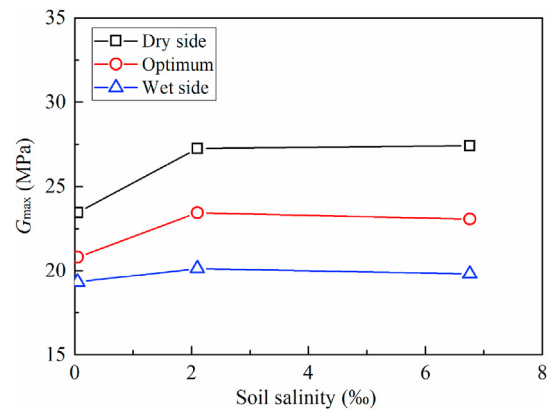


Fig. 6. Salinity effect on small-strain shear modulus.

given soil salinity, the chosen points on dry and wet sides corresponded to the same dry density. The corresponding compactness which was the ratio of target dry density to maximum dry density was 98.8% for soil without salt and 98.2% for soils with soil salinities of 2.1‰ and 6.76‰ that were almost similar.

3.2. Matric suction

Fig. 5 depicts the changes in matric suction of compacted samples on dry and wet sides and at optimum state. It appears that all the points lay on one unique line, suggesting that the matric suction was highly related to the water content of samples, whereas the salinity had no significant effect on matric suction. This was in good agreement with previous results from Miller and Nelson (1993), Leong et al. (2007), Sreedeeep and Singh (2011) and Zhang et al. (2017). It was also observed that, for the dry samples with the same water content, the matric suctions of saltless and saline samples were quite close, while the matric suctions of saltless samples compacted at optimum state and on wet side were

Table 4 Properties of compacted samples.

$r'$ (‰)	State	Water content (%)	Dry density (Mg/m <sup>3</sup> )	Degree of saturation (%)	Compactness (%)
0	Dry side	15.2	1.69	68	98.8
	Optimum	16.5	1.71	76	100
	Wet side	18.2	1.69	82	98.8
2.1, 6.76	Dry side	15.2	1.65	63	98.2
	Optimum	17.5	1.68	77	100
	Wet side	19.7	1.65	82	98.2

noticeably higher than those of saline samples with soil salinities of 2.1‰ and 6.76‰.

3.3. Small-strain shear modulus

The  $G_{max}$  was affected by many factors, including soil properties, compaction state, compaction stress and matric suction (Ng et al., 2009). As shown in Table 4, the compactness was almost the same for samples having different salinities which were compacted on dry and wet sides and at optimum state, respectively, although the dry density of saltless samples was higher than that of saline samples. Moreover, as mentioned before, all samples were subjected to the same compaction pressure of around 2200 kPa. This implied that the effects of compactness (or dry density) and compaction energy on  $G_{max}$  can be ignored. Thus, there were remaining two factors affecting the  $G_{max}$  values: one was matric suction, and the other one was salinity. The variations of  $G_{max}$  with soil salinity are plotted in Fig. 6. For the samples compacted on the dry side, the matric suction was rather close (Fig. 5). Thus, the soil salinity was the sole factor to influence the  $G_{max}$  for the dry samples. As shown in Fig. 6, the  $G_{max}$  for dry samples decreased with the decrease of soil salinity from initial value of 2.1‰ to zero, whereas it kept almost constant with the increase of soil salinity from 2.1‰ to 6.76‰. The same trend of  $G_{max}$  variations was also observed for the samples compacted at optimum state and on wet side. However, in that case, the difference of  $G_{max}$  between the saltless and saline samples was controlled by both matric suction and soil salinity. For the samples compacted at optimum state and on wet side, the matric suctions for saltless samples were higher than those of samples with soil salinities of 2.1‰ and 6.76‰ (Fig. 5). Ng et al. (2008, 2017) and Heitor et al. (2013) indicated that the  $G_{max}$  increased with increasing matric suction. This implies that, if the salinity effect was neglected, the  $G_{max}$  for the saltless samples should be higher than those of samples with soil salinities of 2.1‰ and 6.76‰, due to their higher matric suction. Nevertheless, it was observed that  $G_{max}$  for the samples compacted at optimum state and on wet side decreased with the decrease of soil salinity from 2.1‰ to zero, suggesting that the decrease of salinity led to a reduction of  $G_{max}$  that prevailed the increase of  $G_{max}$  as matric suction increased. This resulted in a decrease of salinity effect on  $G_{max}$  from dry side to wet side, due to the balance of the increase of  $G_{max}$  with increasing matric suction and the decrease of  $G_{max}$  with decreasing salinity for optimum and wet side samples. Specifically, as soil salinity decreased from 2.1‰ to zero, the  $G_{max}$  decreased from 27.24 MPa to 23.45 MPa (14%) for samples compacted on dry side, from 23.44 MPa to 20.8 MPa (11%) for samples compacted at optimum state, and from 20.13 MPa to 19.32 MPa (4%) for samples compacted on wet side. This salinity effect on  $G_{max}$  was in full agreement with the changes of compaction curves observed previously - the salinity effect on compaction curves also decreased from dry side to wet side (Fig. 4).

3.4. Microstructure investigation

The cumulative curves and corresponding derived curves are presented in Fig. 7 for the samples compacted on dry side, Fig. 8 for the samples compacted at optimum state, and Fig. 9 for the samples compacted on wet side. Based on the MIP results and the hypothesis that the water is contained in small pores (Wan et al., 1995; Romero et al., 2011), the water ratio (i.e. void ratio of water-saturated pores,  $e_w = wG_s$ ) and delimiting diameter between water-saturated pores and dry pores were determined, as shown in Figs. 7a, 8a and 9a. The corresponding distributions of water-saturated pores are presented in Figs. 7b, 8b and 9b. It appears from the cumulative curves that the total intruded void ratios were

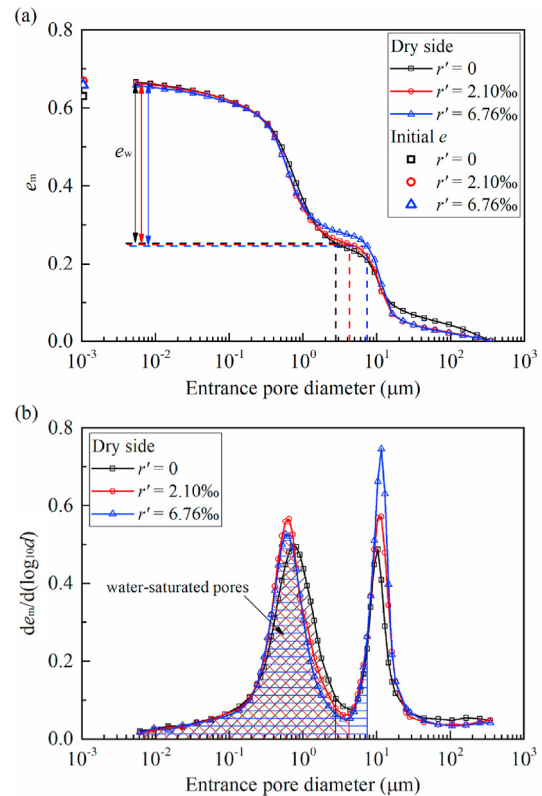


Fig. 7. MIP results of samples compacted on dry side: (a) Cumulative intrusion curves; and (b) Derived curves.

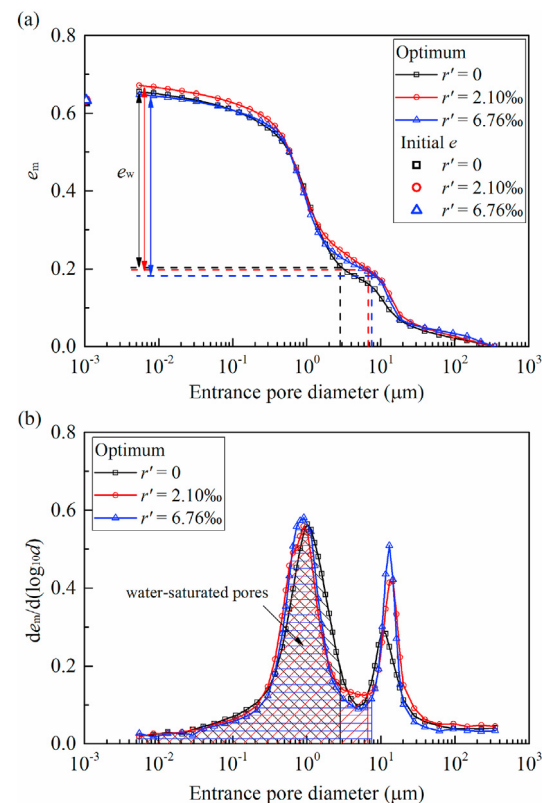


Fig. 8. MIP results of samples compacted at optimum water content: (a) Cumulative intrusion curves; and (b) Derived curves.

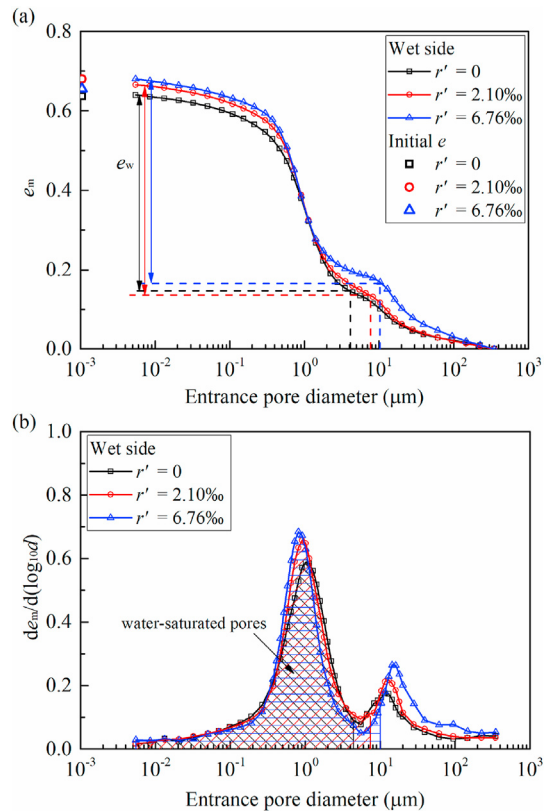


Fig. 9. MIP results of samples compacted on wet side: (a) Cumulative intrusion curves; and (b) Derived curves.

relatively close to the initial void ratio of samples which were determined from sample dimension. The total intruded void ratios were almost similar for dry samples having different salinities. Concerning the optimum and wet samples, the total intruded void ratios of saltless samples were slightly lower than that of saline samples, which might be due to its relative higher dry density of saltless samples. As shown in Figs. 7b, 8b and 9b, the derived curves exhibited typical bi-modal characteristics not only for the samples compacted on dry side and at optimum state as usually observed, but also for the samples compacted on wet side of optimum, with a population of micro-pores and a population of macro-pores. For all samples on dry and wet sides and at optimum state, the water was mostly adsorbed and held in the micro-pores, leaving the most of macro-pores being dry. As for the dry samples, with decreasing soil salinity from the initial value of 2.1‰ to zero, the modal size of micro-pores increased from 0.63 μm to 0.78 μm and that of macro-pores decreased from 11.63 μm to 10.23 μm, while there was no significant change when the soil salinity increased from 2.1‰ to higher value of 6.76‰ (Fig. 7b). The similar results were obtained on the samples compacted at optimum state: as the soil salinity decreased from 2.1‰ to zero, the modal size of micro-pores shifted from 0.91 μm to 1.03 μm and that of macro-pores shifted from 13.17 μm to 10.86 μm, whereas the modal sizes of both macro- and micro-pores had no significant change with increasing soil salinity to 6.76‰ (Fig. 8b). As for the wet samples, the modal size of micro-pores increased from 0.91 μm to 1.05 μm and that of macro-pores decreased from 12.91 μm to 11.82 μm with decreasing soil salinity from 2.1‰ to zero, while the modal size of micro-pores decreased slightly and that of macro-pores increased with increasing soil salinity from initial value of 2.1‰ to 6.76‰ (Fig. 9b). Besides, as salinity increased, an increase in the frequency of macro-pores was observed on all kinds of samples.

#### 4. Discussion

Microstructure of compacted soil was significantly dependent on the compacted water content (Delage et al., 1996). For silty soil, on dry side, the clay coated the surface of grains and the compaction cannot significantly deform the aggregates due to the high suction effect. This led to an aggregated structure characterised by bi-modal pore size distributions. On wet side, the clay fraction formed a continuous or more compact matrix around the sand or silt grains and the clay paste was able to fill the macro-pores. In that case, a uni-modal pore population was usually identified. Thus, it was not a common result that the wet samples presented aggregated structure with a high population of micro-pores and a small population of macro-pores, as shown in Fig. 9b. Russo and Modoni (2013) also observed the bi-modal pore size distribution characteristics for alluvial silty sand with only 13% clay-size fraction which was compacted on wet side. Burton et al. (2014) indicated that the wet samples can also present aggregated structure if their compaction energy and degree of saturation were low. For the tested silty soil, the clay-size fraction was only 17%. The degree of saturation of compacted samples was around 82% that was close to the value at optimum state (78%). Thus, the low clay fraction and the degree of saturation close to the one at optimum state might be the possible reasons for the bi-modal pores size distribution characteristics observed on wet samples that the limited clay paste could not form a continuous matrix to fill all macro-pores.

As observed in Figs. 7b, 8b and 9b, the modal size of micro-pores decreased, while the modal size and frequency of macro-pores increased with increasing soil salinity from zero to 2.1‰ and 6.76‰. The changes in micro-pores were mainly attributed to the salinity effect which led to a decrease of diffused double layer thickness of clay minerals (Ravi and Rao, 2013; Thyagaraj and Salini, 2015). The microstructure of compacted silty soil was characterised by sand or silt grain skeleton with clay particles coating these grains, and these grains and clay particles formed aggregates (Delage et al., 1996; Lemaire et al., 2013). The pores within these aggregates were identified as micro-pores and the pores between these aggregates were regarded as macro-pores. As salinity increased, the thickness of diffused double layer decreased (Sridharan and Jayadeva, 1982; Sridharan and Prakash, 2000), leading to a reduction of micro-pore size for clay particles. Such decrease of diffused double layer thickness further induced an increase of macro-pore size and its frequency (Yilmaz et al., 2008; Shariatmadari et al., 2011). In addition, the frequency of macro-pores was also affected by the dry density: the higher the dry density, the lower the frequency of the macro-pores (Romero, 2013). It was noting that the salinity effect on the pore size distributions (especially for micro-pores) was visible with increasing salinity from zero to 2.1‰ while this salinity effect was negligible when the salinity increased from 2.1‰ to 6.76‰. This might be attributed to the low clay fraction and its less active clay minerals (10.8% illite, 3.6% chlorite and 1.3% kaolinite) in the tested silty soil limiting the compression of diffused double layer at higher salinity (Ying et al., 2020), as its thickness already decreased significantly at 2.1‰ soil salinity. As most water was contained in the micro-pores, the relationship between water content and matric suction was mainly governed by the micro-pores while the dry macro-pores which were easily affected by dry density played a negligible role. Thus, the points of water content and matric suction converged to one unique line despite different dry densities (Fig. 5). This was consistent with the results obtained by Heitor et al. (2013), showing that when the soil water retention properties of compacted silty sand were expressed in terms of water content and matric suction, the matric suctions were independent of dry density. The salinity effect on the matric suction



was slight as observed in Fig. 5, which might be attributed to the visible but insignificant changes of micro-pores induced by salinity.

As soil microstructure changed with increasing salinity, the  $G_{\max}$  of saline samples was expected to be higher than that of the samples without salt (Fig. 6). Since the distance between interlayers of clay decreased with the reduction of diffused double layer thickness, the inter-particle repulsive forces decreased, resulting in an increase of net attractive forces which may make clay particles attract each other and agglomerate (Warkentin and Yong, 1962; Sridharan et al., 2002; Israelachvili, 2011). This association enhanced soil strength (Warkentin and Yong, 1962; Sridharan et al., 2002). As far as the compaction behaviour was concerned, for the same compaction energy, a stiffer soil with higher  $G_{\max}$  presented higher resistance to compaction. As a result, a lower maximum dry density of saline samples was obtained (Fig. 4). Meanwhile, more water was needed to destroy soil aggregates for stiffer soils. Thus, the optimum water content increased for saline soil (Fig. 4). However, the optimum degree of saturation seemed to be insensitive to salinity (Table 4), even though the microstructure and stiffness varied. This was consistent with the observations made by Tatsuoka (2015) and Tatsuoka and Correia (2018). They reported that the optimum degree of saturation of compacted soil was nearly 82%, independent of soil type and compaction energy level. It can be deduced from Eq. (6) that, for the saline soil, the balance between the increased optimum water content and the decreased maximum dry density led to a negligible change in optimum degree of saturation.

Regarding the saline samples with different salinities, they had rather close  $G_{\max}$  and Proctor compaction curves. It was consistent with the changes in microstructure that these behaviours varied significantly when the soil salinity increased from zero to 2.1‰, while these variations were slight with increasing soil salinity from 2.1‰ to 6.76‰, due to the limited salinity effect through changes of diffused double layer thickness at higher salinity. Similar observations were made by Ajalloeian et al. (2013): the shear strength and friction angle increased and then kept almost constant with increasing salinity in soils with only 28% clay-size fraction. It was also comparable to the results of saturated bentonite whose residual shear strength increased significantly in the range from 0 mol/L to 0.5 mol/L NaCl solution and then had negligible variations for concentrations larger than 0.5 mol/L (Di Maio, 1996).

## 5. Conclusions

To better understand the salinity effect on the compaction behaviour of silty soil, standard Proctor compaction test, filter paper method and bender element test coupled with MIP test were conducted on a silty soil with different salinities. The obtained results allowed the following conclusions to be drawn:

- (1) The pore size distribution curves presented bi-modal characteristics not only for the samples compacted on dry side and at optimum state as usually observed but also for the samples compacted on wet side. The smaller quantity of macro-pores for wet samples can be attributed to the low clay-size fraction whose paste could not form a continuous matrix to fill all macro-pores, and to the degree of saturation close to that of optimum.
- (2) The pore size distribution of compacted samples also depended on soil salinity. For the samples with soil salinities of 2.1‰ and 6.76‰, the modal size of micro-pores shifted to smaller values, whereas the modal size of macro-pores shifted to larger values than that of samples without salt. This can be explained by the decrease of diffused double layer thickness of clay particles, leading to a reduction of the

modal size of micro-pores and further inducing increases of the frequency and modal size of macro-pores.

- (3) Due to the modification of microstructure associated with salinity, the samples with soil salinities of 2.1‰ and 6.76‰ exhibited higher  $G_{\max}$  than that of samples without salt. This observation was not only made on dry samples with similar matric suctions, but also for the samples compacted at optimum state and on wet side, whose matric suctions were slightly different, due to the difference in remoulded water content. The higher  $G_{\max}$  obtained for saline soil could be explained by the fact that, as salinity increased, the net attractive forces increased with the reduction of diffused double layer thickness that made clay particles attract each other and agglomerate, giving rise to an increase of  $G_{\max}$ .
- (4) The saline soil exhibited higher  $G_{\max}$  and became less compactible. Thus, for the same compaction energy, the saline soil exhibited lower maximum dry density and higher optimum water content. Besides, the effect of salinity on compaction behaviour and  $G_{\max}$  decreased while passing from dry side to wet side.
- (5) The Proctor compaction curves and  $G_{\max}$  of saline samples with different soil salinities were rather similar. This could be attributed to the low clay fraction and their mineral compositions (illite, chlorite and kaolinite), which limited the salinity effect through changes in diffused double layer thickness of clay particles.

## Declaration of competing interest

The authors declare that they have no known competing financial interests or personal relationships that could have appeared to influence the work reported in this paper.

## Acknowledgments

The authors would like to thank the China Scholarship Council (CSC), Ecole des Ponts ParisTech (ENPC) and INRAE for their financial support.

## List of symbols

$c$	Salt concentration as the ratio of salt mass to salty water volume
$e_w$	Water ratio
$G_s$	Specific gravity
$G_{\max}$	Small-strain shear modulus
$L_{tt}$	Travel length or tip-to-tip distance between two bender elements
$m$	Wet soil mass
$m_w$	Pure water mass
$m_d$	Solid mass after oven-drying
$r$	Water salinity as the mass ratio of salt to salty water
$r'$	Soil salinity as the mass ratio of salt to dry soil
$\Delta t$	Arrival time of shear wave
$w$	Water content of saltless soil
$w'$	Water content of saline soil
$w_L$	Liquid limit
$w_p$	Plastic limit
$w_f$	Water content of filter paper
$S_r$	Degree of saturation
$\rho$	Density of soil sample
$\rho_d$	Dry density of saltless sample
$\rho'_d$	Dry density of saline sample
$\rho_w$	Liquid density
$v_s$	Shear wave velocity
$\phi_m$	Matric suction

## References

- Abdullah, W.S., Alshibli, K.A., Al-Zou'bi, M.S., 1999. Influence of pore water chemistry on the swelling behaviour of compacted clays. *Appl. Clay Sci.* 15 (5–6), 447–462.
- Abdullah, W.S., Al-Zou'bi, M.S., Alshibli, K.A., 1997. On the physicochemical aspects of compacted clay compressibility. *Can. Geotech. J.* 34 (4), 551–559.
- Abood, T.T., Kasa, A.B., Chik, Z.B., 2007. Stabilisation of silty clay soil using chloride compounds. *J. Eng. Sci. Technol.* 2 (1), 102–110.
- Ajalloeian, R., Mansouri, H., Sadeghpour, A.H., 2013. Effect of saline water on geotechnical properties of fine-grained soil. *Electron. J. Geotech. Eng.* 18, 1419–1434.
- ASTM D4542-95, 2001. Standard Test Method for Pore Water Extraction and Determination of the Soluble Salt Content of Soils by Refractometer. ASTM International, West Conshohocken, PA, USA, 2001.
- ASTM D5298-10, 2010. Standard Test Method for Measurement of Soil Potential (Suction) Using Filter Paper. ASTM International, West Conshohocken, PA, USA, 2010.
- Burton, G.J., Sheng, D.C., Campbell, C., 2014. Bimodal pore size distribution of a high-plasticity compacted clay. *Geotechn. Lett.* 4 (2), 88–93.
- Carteret, R.D., Buzzi, O., Fityus, S., Liu, X.F., 2014. Effect of naturally occurring salts on tensile and shear strength of sealed granular road pavements. *J. Mater. Civ. Eng.* 26 (6), 04014010.
- Cui, Y.J., Delage, P., 1996. Yielding and plastic behaviour of an unsaturated compacted silt. *Geotechnique* 46 (2), 291–311.
- Delage, P., Audiguier, M., Cui, Y.J., Howat, M.D., 1996. Microstructure of a compacted silt. *Can. Geotech. J.* 33 (1), 150–158.
- Di Maio, C., 1996. Exposure of bentonite to salt solution: osmotic and mechanical effects. *Geotechnique* 46 (4), 695–707.
- Di Maio, C., Santoli, L., Schiavone, P., 2004. Volume change behaviour of clays: the influence of mineral composition, pore fluid composition and stress state. *Mech. Mater.* 36 (5–6), 435–451.
- Durotoye, T.O., Akinmusuru, J.O., Ogbiye, A.S., Bamigboye, G.O., 2016. Effect of common salt on the engineering properties of expansive soil. *Int. J. Eng. Technol.* 6 (7), 233–241.
- Heitor, A., Indraratna, B., Rujikiatkamjorn, C., 2013. Laboratory study of small-strain behaviour of a compacted silty sand. *Can. Geotech. J.* 50 (2), 179–188.
- Israelachvili, J.N., 2011. *Intermolecular and Surface Forces*, third ed. Academic Press.
- Lemaire, K., Deneele, D., Bonnet, S., Legret, M., 2013. Effects of lime and cement treatment on the physicochemical, microstructural and mechanical characteristics of a plastic silt. *Eng. Geol.* 166, 255–261.
- Leong, E.C., Widiastuti, S., Lee, C.C., Rahardjo, H., 2007. Accuracy of suction measurement. *Geotechnique* 57 (6), 547–556.
- Liu, J.Y., Zhang, L.J., 2014. The microstructure characters of saline soil in Qarhan Salt Lake area and its behaviours of mechanics and compressive strength. *Arabian J. Sci. Eng.* 39 (12), 8649–8658.
- Miller, D.J., Nelson, J.D., 1993. Osmotic suction as a valid stress state variable in unsaturated soil mechanics. In: *Unsaturated Soils*. American Society of Civil Engineers (ASCE), pp. 64–76.
- Mitchell, J.K., Soga, K., 2005. *Fundamentals of Soil Behaviour*, third ed. John Wiley & Sons, Inc.
- Moore, R., 1991. The chemical and mineralogical controls upon the residual strength of pure and natural clays. *Geotechnique* 41 (1), 35–47.
- NF P18-837, 1993. Standard for Special Products for Hydraulic Concrete Construction - Hydraulic Binder Based Needling And/or Sealing Products - Testing of Resistance against Seawater And/or Water with High Sulphate Contents. AFNOR.
- NF P94-056, 1996. Standard Test for Soils Investigation and Testing - Granulometric Analysis - Dry Sieving Method after Washing. AFNOR.
- NF P94-057, 1992. Standard Test for Soils Investigation and Testing - Granulometric Analysis - Hydrometer Method. AFNOR.
- NF P94-093, 1999. Standard Test for Soils Investigation and Testing - Determination of the Compaction Characteristics of a Soil - Standard Proctor Test - Modified Proctor Test. AFNOR.
- Ng, C.W.W., Yung, S.Y., 2008. Determination of the anisotropic shear stiffness of an unsaturated decomposed soil. *Geotechnique* 58 (1), 23–35.
- Ng, C.W.W., Xu, J., Yung, S.Y., 2009. Effects of wetting-drying and stress ratio on anisotropic stiffness of an unsaturated soil at very small strains. *Can. Geotech. J.* 46 (9), 1062–1076.
- Ng, C.W.W., Baghbanrezvan, S., Sadeghi, H., Zhou, C., Jafarzadeh, F., 2017. Effect of specimen preparation techniques on dynamic properties of unsaturated fine-grained soil at high suctions. *Can. Geotech. J.* 54 (9), 1310–1319.
- Noorany, I., 1984. Phase relations in marine soils. *J. Geotech. Eng.* 110 (4), 539–543.
- Ravi, K., Rao, S.M., 2013. Influence of infiltration of sodium chloride solutions on SWCC of compacted bentonite-sand specimens. *Geotech. Geol. Eng.* 31 (4), 1291–1303.
- Reitemeier, R.F., 1946. Effect of moisture content on the dissolved and exchangeable ions of soils of arid regions. *Soil Sci.* 61 (3), 195–214.
- Romero, E., Della Vecchia, G., Jommi, C., 2011. An insight into the water retention properties of compacted clayey soils. *Geotechnique* 61 (4), 313–328.
- Romero, E., 2013. A microstructural insight into compacted clayey soils and their hydraulic properties. *Eng. Geol.* 165, 3–19.
- Russo, G., Modoni, G., 2013. Fabric changes induced by lime addition on a compacted alluvial soil. *Geotechn. Lett.* 3 (2), 93–97.
- Sarkar, G., Siddiqua, S., 2016. Effect of fluid chemistry on the microstructure of light backfill: an X-ray CT investigation. *Eng. Geol.* 202, 153–162.
- Shariatmadari, N., Salami, M., Fard, M.K., 2011. Effect of inorganic salt solutions on some geotechnical properties of soil-bentonite mixtures as barriers. *Int. J. Civ. Eng.* 9 (2), 103–110.
- Siddiqua, S., Blatz, J., Siemens, J., 2011. Evaluation of the impact of pore fluid chemistry on the hydromechanical behaviour of clay-based sealing materials. *Can. Geotech. J.* 48 (2), 199–213.
- Sreedeeep, S., Singh, D.N., 2011. Critical review of the methodologies employed for soil suction measurement. *Int. J. Geomech.* 11 (2), 99–104.
- Sridharan, A., Jayadeva, M.S., 1982. Double layer theory and compressibility of clays. *Geotechnique* 32 (2), 133–144.
- Sridharan, A., Prakash, K., 2000. Percussion and cone methods of determining the liquid limit of soils: controlling mechanisms. *Geotech. Test J.* 23 (2), 236–244.
- Sridharan, A., AEI-Shafei, A., Miura, N., 2002. Mechanisms controlling the undrained strength behaviour of remolded Ariake marine clays. *Mar. Georesour. Geotechnol.* 20 (1), 21–50.
- Tang, A.M., Vu, M.N., Cui, Y.J., 2011. Effects of the maximum soil aggregates size and cyclic wetting-drying on the stiffness of a lime-treated clayey soil. *Geotechnique* 61 (5), 421–429.
- Tatsuoka, F., 2015. Compaction characteristics and physical properties of compacted soil controlled by the degree of saturation. In: *Proceedings of the 15th Pan-American Conference on Soil Mechanics and Geotechnical Engineering and 6th International Conference on Deformation Characteristics of Geomaterials*, Buenos Aires, pp. 40–76.
- Tatsuoka, F., Correia, A.G., 2018. Importance of controlling the degree of saturation in soil compaction linked to soil structure design. *Transport. Geotech.* 17, 3–27.
- Thyagaraj, T., Salini, U., 2015. Effect of pore fluid osmotic suction on matric and total suctions of compacted clay. *Geotechnique* 65 (11), 952–960.
- Tiwari, B., Tuladhar, G.R., Marui, H., 2005. Variation in residual shear strength of the soil with the salinity of pore fluid. *J. Geotech. Geoenviron. Eng.* 131 (12), 1445–1456.
- Truong, Q.H., Lee, C., Kim, Y.U., Lee, J.S., 2012. Small strain stiffness of salt-cemented granular media under low confinement. *Geotechnique* 62 (10), 949–953.
- Wan, A.W.L., Gray, M.N., Graham, J., 1995. On the relations of suction, moisture content and soil structure in compacted clays. In: *Proceedings of the 1st International Conference on Unsaturated Soils*. A.A. Balkema, Paris.
- Wang, Y.J., Benahmed, N., Cui, Y.J., Tang, A.M., 2017. A novel method for determining the small-strain shear modulus of soil using the bender elements technique. *Can. Geotech. J.* 54 (2), 280–289.
- Wang, Y.J., Cui, Y.J., Benahmed, N., Tang, A.M., Duc, M., 2020. Changes of small strain shear modulus and suction for a lime-treated silt during curing. *Geotechnique* 70 (3), 276–280.
- Warkentin, B.P., Yong, R.N., 1962. Shear strength of montmorillonite and kaolinite related to interparticle forces. In: *Proceedings of the 9th National Conference on Clays and Clay Minerals*. Pergamon, pp. 210–218.
- Witteveen, P., Ferrari, A., Laloui, L., 2013. An experimental and constitutive investigation on the chemo-mechanical behaviour of a clay. *Geotechnique* 63 (3), 244–255.
- Yilmaz, G., Yetimoglu, T., Arasan, S., 2008. Hydraulic conductivity of compacted clay liners permeated with inorganic salt solutions. *Waste Manag. Res.* 26 (5), 464–473.
- Ying, Z., Cui, Y.J., Duc, M., Benahmed, N., Bessaies-Bey, H., Chen, B., 2020. Salinity effect on the liquid limit of soils. *Acta Geotechnica*. <https://doi.org/10.1007/s11440-020-01092-7>.
- Ying, Z., Duc, M., Cui, Y.J., Benahmed, N., 2021. Salinity assessment for salted soil considering both dissolved and precipitated salts. *Geotech. Test J.* 44 (1), 130–147.
- Zhang, F.Y., Wang, G.H., Kamai, T., Chen, W.W., Zhang, D.X., Yang, J., 2013a. Undrained shear behaviour of loess saturated with different concentrations of sodium chloride solution. *Eng. Geol.* 155, 69–79.
- Zhang, D.W., Fan, L.B., Liu, S.Y., Deng, Y.F., 2013b. Experimental investigation of unconfined compression strength and stiffness of cement treated salt-rich clay. *Mar. Georesour. Geotechnol.* 31 (4), 360–374.
- Zhang, T.W., Cui, Y.J., Lamas-Lopez, F., Calon, N., Costa D'Aguiar, S., 2018. Compacted soil behaviour through changes of density, suction, and stiffness of soils with remoulding water content. *Can. Geotech. J.* 55 (2), 182–190.
- Zhang, Y., Ye, W.M., Chen, Y.G., Chen, B., 2017. Impact of NaCl on drying shrinkage behavior of low-plasticity soil in earthen heritages. *Can. Geotech. J.* 54 (12), 1762–1774.



**Yu-Jun Cui** obtained his BSc degree in Civil Engineering from Tongji University, China, in 1984, his Master degree in Mechanics applied to Constructions from Ecole des Ponts ParisTech (ENPC), France, in 1989 and his PhD in Unsaturated Soil Mechanics in 1993, also from Ecole des Ponts ParisTech (ENPC). He was employed by ENPC immediately after his PhD as an assistant researcher in the Laboratory of Soil Mechanics (CERMES) now becoming Geotechnique Group of Laboratoire Navier. He passed his Habilitation to Direct Research in Civil Engineering at University of Marne La Vallée, France, in 2000, and obtained the position of professor of ENPC in 2005. He has been Head of Master MSROE (Mécanique des Sols, des Roches et des Ouvrages dans leur Environnement) since 2004. His research interests cover unsaturated soil mechanics, laboratory testing, constitutive modelling, environmental geotechnics, railway geotechnics, nuclear waste disposal, lime/cement stabilized soils, soil-vegetation-atmosphere interaction, compaction of agricultural soils, etc.